First results of LiDAR aided helicopter approaches during NATO DVE-Mitigation trials

Michael Zimmermann[a], m.zimmermann@dlr.de
Christian König[a], christian.koenig@dlr.de
Jens Wolfram[a], jens.wolfram@dlr.de
Martin Gestwa[a], martin.gestwa@dlr.de
Stephanus Klasen[b], stephanus.klasen@hensoldt.net
Andreas Lederle[b], andreas.lederle@hensoldt.net

[a]German Aerospace Center (DLR), Institute of Flight Systems, Braunschweig, Germany
[b]HENSOLDT Sensors GmbH, Immenstaad, Germany

Abstract

Landing a helicopter on unprepared sites can quickly become a challenging task in operational scenarios. Especially when environmental factors reduce the available visual cues for the pilot, the risk of disorientation increases. Motivated by avoiding accidents occurring in these Degraded Visual Environments (DVE), the NATO program for DVE-Mitigation (DVE-M) supports international efforts in the development of systems for enhanced situational awareness during DVE. A workgroup of the German Aerospace Center (DLR) and HENSOLDT Sensors GmbH participated at flight trials of the European NATO DVE-M campaign in Manching with DLRs highly modified research helicopter. The state of a system currently being under development was presented which combines eyes-out tunnel-in-the-sky symbology (SferiAssist®) with dynamic path updates based on a laser sensor. Details of four flights during the campaign in Manching performed in February 2017 are given and discussed in terms of a technical analysis and results of pilot evaluations.

Keywords: Helicopter, approach, hover, LiDAR, obstacle, trajectory, tunnel-in-the-sky

ABBREVIATIONS

ACT/FHS	Advanced Control Technology/ Flying Helicopter Simulator
AVES	Air Vehicle Simulator
DSM	Digital Surface Model
DVE	Degraded Visual Environments
EP	Evaluation Pilot
FOV	Field of View
FTE	Flight Test Engineer
HDD	Head Down Display
HMI	Human Machine Interface
HMS/D	Helmet Mounted Sight Display
LiDAR	Light Detection and Ranging
MFD	Multi-Function Display
MSL	Mean Sea Level
SP	Safety Pilot
WTD-61	Wehrtechnische Dienststelle 61

1 INTRODUCTION

The approach-to-landing/hover phase of helicopters to unprepared landing sites in unknown terrain may introduce high operational risks. A study of the U.S. Joint Helicopter Safety Analysis Team [1] states that out of 523 analyzed accidents in the years 2000, 2001 and 2006, 7% (36) occurred during approach and 21% (108) during the landing phase. Similar results are obtained by a study of the European Helicopter Safety Team (EHEST) [2], showing that 28% of 487 analyzed accidents from 2005-2010 occurred in these phases of flight. As soon as the outside visual cues deteriorate - which is described as Degraded Visual Environment (DVE) - the pilot's workload and the probability of potential loss of situational awareness both increase significantly. DVE is one of the major drivers for accidents during the approach and landing of helicopters, especially in military operations.

The following paper is structured in seven sections. The first section gives a short summary of related measures solving the problems arising through DVE, followed by a description of the DVE-Mitigation (DVE-M) program and related work at DLR. In section two, the general system design is outlined, including details on sensors and procedures. The third section describes the scenario and preparation of the NATO-DVE Mitigation flight trials in February 2017. Section four discusses the evaluation, and section five summarizes results of these flights, divided into technical and pilot-centered subsections. The final sections six and seven give conclusions and point out future work.

1.1 State of the art

Possible solutions to the DVE problem have been examined by a study group of the NATO Industrial Advisory Group (NIAG). According to their final report [3], DVE solutions were subdivided into four

classes, each containing a visualization component and sensor systems of increasing complexity:

Class 4 systems are the least capable systems, solely relying on database information.

Class 3 systems provide additional real-time information by using passive imaging sensors with TV-like or Forward Looking Infrared (FLIR) cameras.

Class 2 systems add active real-time sensors like LiDAR to the sensing package which are combined with the class 3/4 sensing approaches.

Class 1: systems shall combine the sensed information with the flight control system, allowing the pilot to select between autonomous or manual system operations.

Systems relying on pre-stored information only (class 4) are prone to errors for several reasons as discussed by Münsterer et al. [4]. While digital surface models derived from satellite measurements (e.g. SRTM, ASTER or TanDEM-X) or topographical map digitized data may provide large coverage of the world surface, using these datasets for close-to-ground navigation imposes risks due to their age, limited accuracy or partial incompleteness.

A recent accident of a Sikorsky S-92 on a Search and Rescue mission near Ireland reveals shortcomings in such database-only systems. According to the preliminary report [5], the terrain model within the helicopters Enhanced Ground Proximity warning system (EGPWS) did neither include the island in the helicopters flight path in its full height, nor the lighthouse on top of it, hence no cues were triggered by the system.

For near ground operations like approaches to hover or landing in DVE, active real-time sensing or better systems are recommended (class 2) in the NIAG report [3]. The comparison of such systems during flight evaluations was part of the DVE-Mitigation program.

1.2 DVE Mitigation program

In order to increase the operational capabilities and the survivability in DVE scenarios, the DVE-Mitigation program was introduced by the U.S. Army Research, Development and Engineering Command (RDECOM). Exchange of technical information with other NATO countries is organized through workgroups focusing on vertical lift (JCG-VL) and DVE (NIAG-193). A comprehensive overview of the NATO related activities can be found in Ref. [6]. Besides collecting valuable technical data in relevant scenarios, feedback from evaluation pilots for specific systems is another outcome of this program.

First flight trials within the DVE-M program were performed in September 2016 at Yuma Proving ground, focusing primarily on brown-out situations. Detailed results of these trials are published by Szoboszlay et al. in Ref. [7].

The first of two parts of the European NATO DVE-M campaign was scheduled for February 2017 and hosted by the German armed forces at the Bundeswehr Technical Center for Aircraft and Aeronautical Equipment (WTD-61) in Manching, Germany. Here, scenarios beyond brown-out were to be considered. The second part of the campaign was hosted by the Swiss armed forces in Alpnach, focusing on snow and white-out.

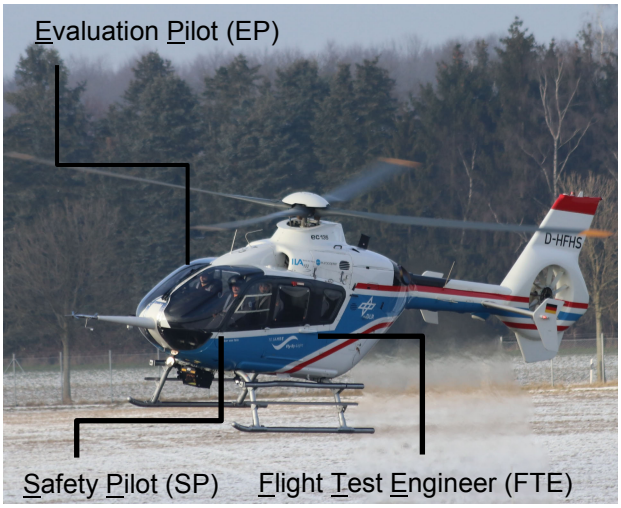

Figure 1: ACT/FHS in NATO DVE-M trial configuration.

Due to experience with respect to pilot assistance systems, a workgroup from DLR and HENSOLDT participated in the DVE-M campaign in Manching, using DLR's research rotorcraft named Active Control Technology/Flying Helicopter Simulator (ACT/FHS) seen in Figure 1. A short summary of past related work is given in the next section.

1.3 Related work at DLR

The ACT/FHS, a highly modified EC135 rotorcraft, is in service since 2002 [8]. The major modification of the helicopter is the replacement of its mechanical control system by a full-authority fly-by-wire/fly-by-light system, divided in a safe and flexible part:

- A quadruplex core system fulfilling airworthiness safety standards.
- A simplex experimental system including a flight control computer and optional equipment like sensors or Human Machine Interfaces (HMI).

Due to the two-sided architecture and a safe concept of operation, experimental software does not have to fulfill airworthiness standards.

Experimental flights are always conducted with a crew of three onboard, see Figure 1. The Evaluation Pilot (EP) seated in the front right performs the

experiment. The Safety Pilot (SP) seated on the left side monitors control inputs and may, at any time, end the experiment and return to direct control. The Flight Test Engineer (FTE), seated in the back, usually leads through the test-points and observes real-time data.

During the project *ALLFlight (Assisted Low Level Flight and Landing on unprepared Sites)*, lasting from 2008 until mid of 2013, the ACT/FHS's experimental system was extended by a sensor suite including four forward looking sensors (IR, TV, LiDAR, Radar) and a military grade Helmet Mounted Sight and Display (HMS/D). While details of the most relevant components are given in the next section, the reader may be referred to a more detailed overview by Greiser et al. [9]. Referring to the DVE classes mentioned in section 1.1, the established infrastructure of components for sensing, flight controls and HMI fulfills the boundary conditions for DVE solutions up to class 1.

In parallel, a new DLR flight simulator named Air Vehicle Simulator (AVES) was built and went operational in early 2014 [10]. Within AVES, a replication of the ACT/FHS's cockpit is present, including a replication of its experimental system. It contains a flexible sensor simulation [11] and is used for hardware-in-the-loop system integration, pilot studies and flight test preparation.

One of the first projects incorporating a majority of the available components was a cooperative work between DLR and HENSOLDT within the project *Transition to Hover (TtH),* presented in [12] by Wolfram et al. One of the goals of this collaborative effort was to combine the HMI and sensing components of HENSOLDTs product family Sferion® with path planning and flight control laws developed by DLR. Within the scope of *TtH*, the combined system was integrated into the simulation environments of both partners. Pilot feedback was collected during several workshops and flights in local scenery in Braunschweig in late 2015. Following the lessons learned during *TtH,* the collaboration was extended within *Transition from forward flight to Hover (T2H).* In mid of December 2016, the *T2H* team was asked to participate in the DVE-M campaign at Manching, leaving a preparation time of practically less than four weeks.

Due to prevailing technical constraints, the experimental flight control laws could not be used during the campaign and the EPs had to fly the helicopter without stability augmentation or autopilot modes.

2 SYSTEM DESCRIPTION

The evaluated system supports the pilot primarily during the final approach phase to a geo-referenced hover point. A general block diagram with the involved components is shown in Figure 3, outlining the communication in the distributed system.

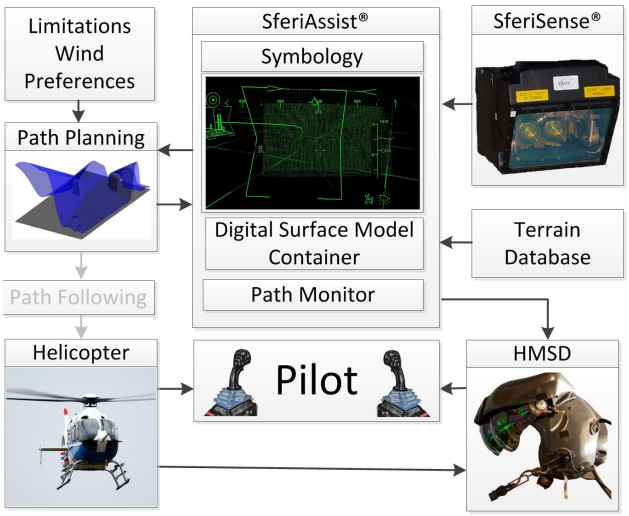

Figure 3: General block diagram

After a hover point was manually set by the pilot, an initial flight path is calculated by the *Path Planning* module. Referring to the blocks in Figure 3, four features related to the intended flight path support the pilot during the approach.

First, the proposed solution is shown to the pilot with visual cues in a HMS/D using SferiAssist® *Symbology*. The pilot may either follow the cues manually or hand over the controls to the autopilot (*Path Following*). While following the flight path, real-time data by the SferiSense® sensor is used by the *Path Monitor* which may declare a flight path as unsafe due to nearby obstacles. A new flight path can be determined by the *Path Planning* module based on an up-to-date Digital Surface Model (DSM).

2.1 Sensor

The two axis scanning laser sensor seen in Figure 2 is a SferiSense® 300. It is eye-safe and measures distances by using flight-time of emitted light pulses.

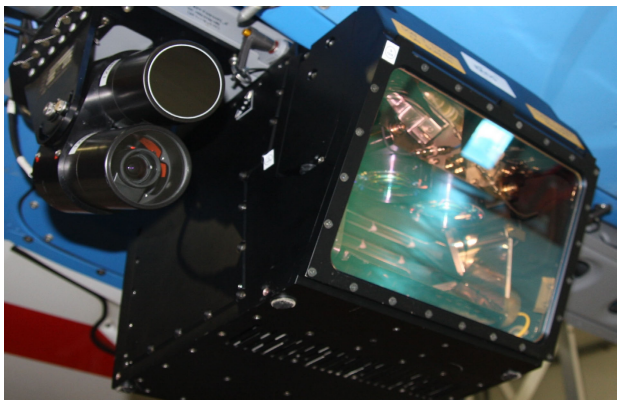

Figure 2: SferiSense® 300 (right) and TV and IR cameras (both used for recording only)

Development of this technology reaches back to the early 1990s, documented by Eibert et al. [13]. A detailed description including a derivation of the detection probability for wires is given by Schulz et al. in Ref. [14]. First systems were fielded on civil helicopters at the German Border Police.

The range of detection is 50 m to 1000 m in a 31.5° (horizontal) x 32° (vertical) field of view (FOV). The vertical resolution of 200 lines is higher than the lateral with 95 rows, outputted at 2 frames per second. A perspective view of the FOV geometry for a typical height above ground of 100 m is shown in Figure 4.

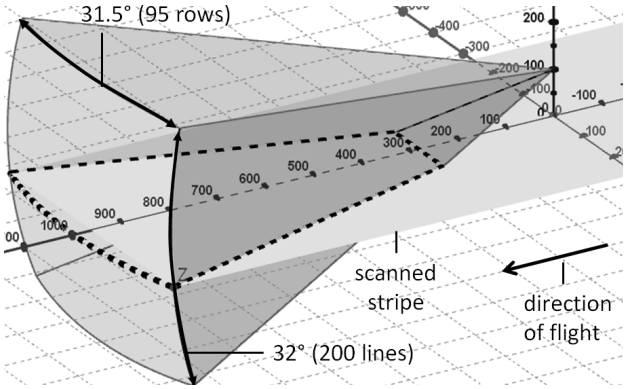

Figure 4: SferiSense® 300 field of view in 100 m above ground level

The scan volume is tilted 5° down and bounded by four body-fixed planes and a sphere, illustrated as grey sectors in Figure 4. In straight and level flight, the intersection of this volume with the ground, shown as dotted, thick outline in Figure 4, accumulates to a stripe of less than 600 m in width which is also depicted in the figure.

Additionally, a military version was fielded at the NH90 with higher update rates and wider field of view. Both off-the-shelf versions include a two staged onboard filtering and classification process in order to filter false-positives (e.g. sun) and classify leftover points as e.g. ground, poles or wires [15]. Recent progress in dust-cloud filtering in brown-out conditions has been shown by Stelmash et al. [16].

However, the pre-processing of the LiDAR measurements in the ACT/FHS version of the sensor does not include filtering features. Instead, time-stamped point clouds based on the first pulse are outputted. This difference in sensor output allows precise temporal assignment of other time-synchronized data as used by Döhler et al. [17], but is more susceptible to false-positive returns.

2.2 Path updates

In the presented system version, obstacle detection events are triggered once LiDAR samples are within a path-centered safety volume. Figure 5 shows a side view depicting a typical approach of 6°, an obstacle at 100 m distance from a hover location (left, at origin) and the configurable check-volume geometry.

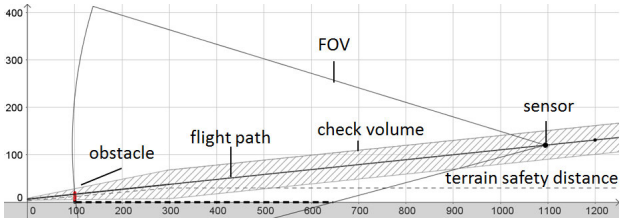

Figure 5: Side view of a straight approach with field of view and safety margins

In the above figure, the sensors distance to the obstacle is set to its theoretical range of 1 km. In this geometry, the obstacle itself takes only a small portion of approximately 1° or 7 lines of the overall vertical FOV of 32° with 200 lines. Once an obstacle enters the FOV and penetrates the check-volume (striped area in Figure 5), a real-time updated DSM is handed over to the path planning module for an update procedure.

Compared to the path-centered safety approach, the planning module currently uses a terrain-centered safety paradigm. The DSM is inflated by an elliptical pattern, allowing varying vertical and horizontal safety distances. It increases in size with further distance from the hover point, shown as dotted lines in Figure 5. Please note that the hover point is displaced upwards by the planning module in case there are obstacles nearby which conflicting the configured safety distances.

Using the inflated DSM, so called visibility hulls based on work published by Srikanth et al. [18] are used to generate a two-segment path to the hover location. An illustration of the process is given in Figure 6 a) to c). In general, visibility hulls represent the lower bound of the visible space from an observing point. Two of these are generated, one from the final hover point (b), and one from the planning start position (a) which is set to a state a predicted time along the active trajectory in order to compensate delays. In Figure 6 a) and b), the observing points are marked with x, the hulls with VH while the spaces are indicated with S and an arrow pointing upwards. The intersection of the spaces $S_{comb}=S_{Hvr}\cap S_{Start}$ contains the subset of space having a direct connection to hover and start point and serves as a search space for possible solutions. In Figure 6 c), its lower bound is depicted as transparent surface.

User defined constraints can be considered by restricting the search to certain areas, e.g. a sector with respect to the hover point. In case the search leaves solutions fulfilling constraints including final approach length, glide path angle or directional

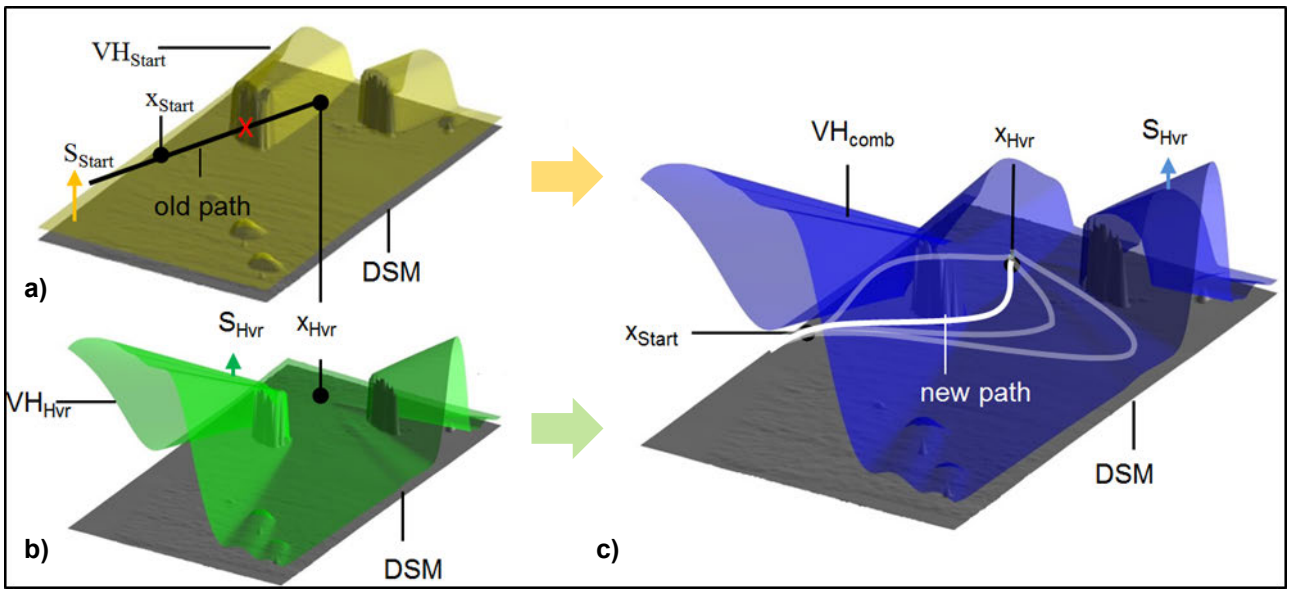

Figure 6: Path update procedure, showing two significant obstacles in Digital Surface Model (DSM)

changes, a new solution with velocity profile with constant deceleration can be proposed to the pilot. The following parameter configuration was used during the campaign and its preparation in the simulator:

- Intended hover height (Skid): **6,1 m (20 ft)**
- Min. length of final approach: **80 m**
- Max. heading change (final turn): **80°**
- Safety distance lateral (0-300 m): **50 m - 65 m**
- Safety distance vertical (0-300 m): **3 m - 30 m**
- Landing Entry Point (LEP)
  - Distance from hover point **1200 m**
  - Height above ground **130 m**
  - Air speed **30 m/s**
- Velocity profile **const. dec.**
- Glide path angle: **6° - 11°**
- Prediction time (for start point) **6 s**

The above mentioned procedure was already applied during flights with vertical avoidance of obstacles and with Head-Down Display guidance, see [19]. With the current computer hardware used for path planning execution, path updates using the procedure above are in the order of less than seconds.

2.3 Human Machine Interface

The visual cues during the evaluation flights to pre-defined hover point were displayed on an Elbit JEDEYE HMS/D. It features a field of view of 80°x40° and a resolution of 1920 pixel by 1200 pixel per eye and contains an integrated magnetic head tracker.

The used symbology is part of SferiAssist®, typically consisting of information which is either earth-fixed (e.g. landing symbology) or head-fixed (e.g. flight state). For the modified symbology set used during the DVE-M campaign, an additional earth-fixed tunnel-in-the-sky was integrated. Images were generated on a high-end graphic computer in the ACT/FHS. A more detailed description of the symbology is given in a later section. Data acquired during one of the flights of the campaign is used to reproduce the symbology in Figure 15 in section 4.3.

Figure 7: Helmet Mounted Sight / Display (Elbit JedEye)

3 PREPARATION

Given the boundary condition of approximately one hour of flight time per pilot, a distinct scenario was needed for familiarization and evaluation. An open space south of Manching airport was identified prior to the NATO DVE-M campaign as a suitable test

area. This area is typically used for training of parachutists, therefore is only referred to as dropping area in this paper.

Two test points were defined. In order to provide a short familiarization of the pilot with the flight dynamics of the ACT/FHS and the symbology in the HMS/D, the first test point was a straight approach (6°) to a hover point with no obstacles within the near vicinity of the intended flight path. The second test point was a straight approach to a hover point, now with an obstacle interfering with the intended approach path. A truck with a man lift of 20 m height was placed 100 m from the hover point, serving as an unmapped obstacle and intended to trigger a flight path update.

A plan view of the dropping area showing the trucks location is depicted in Figure 8. Approaches for three directional variations were defined based on the locally prevailing wind conditions (black arrows) and areas which should be avoided. The resulting approaches are even (free) and odd (obstructed) numbered in Figure 8.

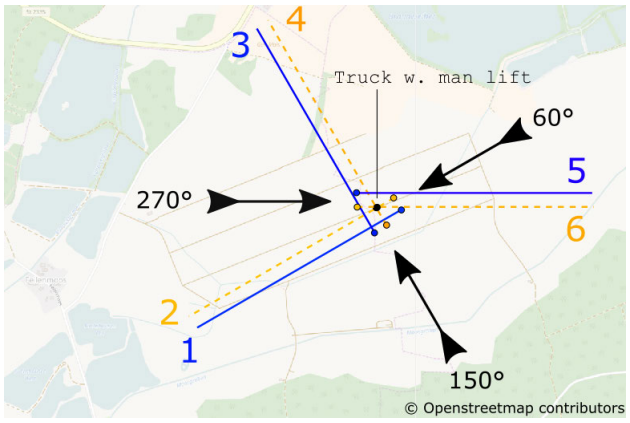

Figure 8: Six predefined approaches at the dropping area south of Ingolstadt/Manching Airport (ETSI)

Since the visual cues in the HMD were only visible to the EP during the flights, all of these six hover points were marked with traffic cones on the ground in order to provide a real-world reference for the SP, seated on the left side.

Two measures were taken to provide the SP a constant visual line of sight to the obstacle during the approaches.

- Free approaches passed the obstacle on its right side.
- The path planning was restricted to search for solutions in a sector to the right side of the obstacle only, intended to force the system to right-turn, left-turn updates.

Based on these restrictions the risk of a potential collision with the truck was minimized.

3.1 Simulation in AVES

In order to verify the expected system behavior before transferring the ACT/FHS to Manching, the scenery was recreated virtually in AVES. A north facing view of the 3D landscape including the obstacle model is shown in Figure 9. During preparation for the campaign, the system was tested in this scenery using the LiDAR simulation, showing that first detections of the truck can be expected around 900 m apart.

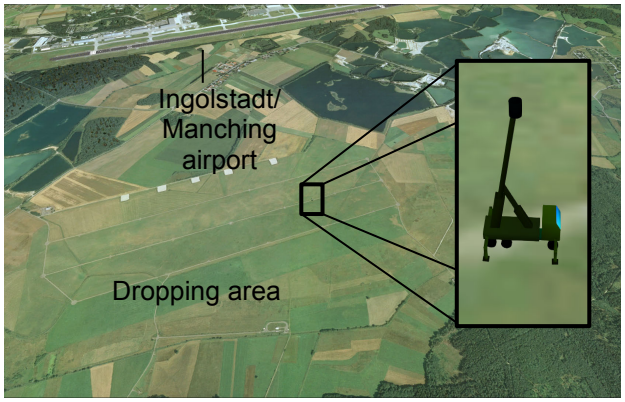

Figure 9: Perspective view of the simulated dropping area and truck in AVES at DLR

During the preparation in the simulator, no HMS/D was available for testing. Therefore, a head-down configuration of SferiAssist® had to be used during system checkout. The situation from a pilot's point of view is shown in Figure 10. The simulated truck is visible above the instrument panel, marked with a black circle in Figure 10 a). The head-down display below shows the symbology for the initial path with orange dotted chevrons indicating the obstacle detection. Figure 10 b) shows the symbology shortly after the path was updated.

a) pre-update b) post-update

Figure 10: SferiAssist® symbology in a head-down configuration during preparation in AVES.

In addition to the pilot's perspective in Figure 10, the data introducing the systems reaction is displayed in Figure 11. In Figure 11 a), the DSM and the initially calculated approach path are shown, shortly after the truck entered the sensors FOV and was identified by the Path Monitor. Note that the z-Direction is stretched by a factor of three. The adjacent Figure 11 b) shows the DSM with applied safety distances and the resulting updated path based on the procedure described in section 2.2.

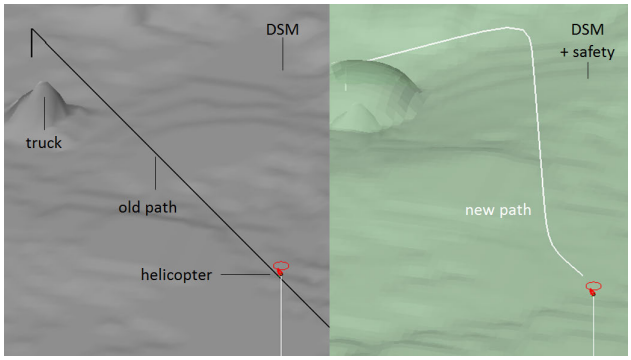

a) pre-update b) post-update

Figure 11: Path update process after an obstacle detection (simulation).

A top view of the flown path is depicted in Figure 12, showing the distance to the obstacle (d_{OBS}) and hover point (d_{LP}) once the obstacle was detected. The closest distance (d_{min}) to the truck is indicated as well. Dotted circles with a radius of 1000, 500 and 100 m are drawn in Figure 12.

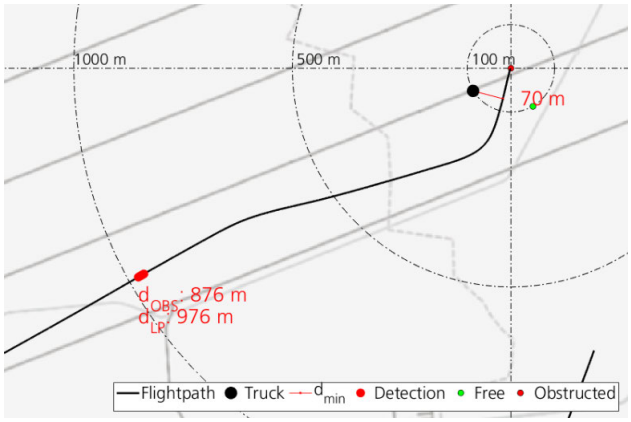

Figure 12: Top view of the flight path with engaged autopilot (simulation)

The velocity profile flown with engaged autopilot (path following mode) is shown in Figure 13. The distances of 100 m, 500 m and 1000 m are marked with vertical lines for comparison. It starts at 30 m/s (TAS) at the start of the final approach and decreases in the initial and updated paths with constant deceleration while approaching the hover point. However, since initially the task of path following was intended to be done by the autopilot, a dedicated speed guidance was not foreseen, hence leaving the choice of speed along the approach to the pilot.

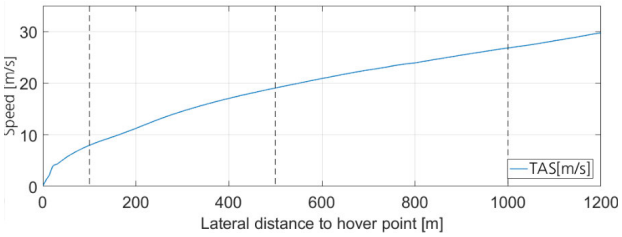

Figure 13: Constant deceleration profile in no wind conditions with engaged path following (simulation)

3.2 Integration

After two integration flights on the 20th and 26th of January in a local obstacle scenery at Braunschweig, the final system set-up for the campaign at Manching was fixed. Due to the time-constrained preparation, compromises in terms of system completeness had to be made:

First, a noticeable lag of the HMS/D symbology was reported by DLRs EPs during fast head movements. In addition, one step in the LiDAR pre-processing was added. As can be seen in Figure 5 (section 2.2), the upper boundary of the FOV may detect objects significantly higher than the helicopters position. In order to avoid problems with low cloud ceilings, LiDAR returns more than 100 ft above the helicopter were to be ignored by the modules for path monitoring and DSM generation. Please note that this solution is specific to the ACT/FHSs version of the SferiSense® LiDAR - both off-the-shelf versions include filtering and classification algorithms (see section 2.1).

3.3 Test on site

When the real truck with extended man lift seen in Figure 14 was available the first time, a final check-out flight was performed with the DLR crew.

Figure 14: The ACT/FHS, shortly before reaching the hover point. © WTD-61

While appearing quite large from an eye level perspective, a narrow structure like this becomes notably harder to see in flat light conditions from an

aerial perspective, especially when it does not stand out with respect to its background in terms of color or texture. The traffic cones seen in the lower part of the image were used as markers for the hover locations. As the system showed the exact same behavior as expected from simulation, the preparations for the upcoming evaluation flights were completed.

4 EVALUATION

The atmospheric conditions on both days as seen in Table 1 lead to the choice of approaches 1 and 2 (see Figure 8) throughout the two days of the campaign.

Table 1: Atmospheric conditions

	Wind	Visibility	Cloud ceiling
2017/02/09	80°/6 kt	>10 km	>1400 ft
2017/02/10	60°/4 kt	> 7 km	>4000 ft

Prior to each flight, the EPs participated in a briefing of the specific safety features of the ACT/FHS and the experiment itself. During system initialization on the ground, a 15 minutes hands-on briefing in the cockpit was given by the SP, followed by take-off and a short transfer flight to the dropping area seen in Figure 8.

Starting in straight and level flight in a downwind parallel to the intended approach, the following action sequence was executed:

- The controls are handed over from SP to EP.
- The FTE initiates an initial flight path calculation.
- The EP accepts the trajectory appearing in his HMS/D by a button on the cyclic stick.
- The EP follows the (possibly changing) flight path until the hover location is reached

When reaching the hover location, the SP took control after an optional short hover and it was proceeded with the next approach. In total, four flights were performed, each lasting approximately one hour with varying number of interruptions due to local traffic.

4.1 Participants

Overall, four pilots participated in evaluation flights with the ACT/FHS, all of them very familiar with the DVE-M program. All of the pilots were holding a qualification as test pilots and were used to glass cockpits and different types of helmet mounted systems. The experience with HMS/D or similar systems ranged from 100 to 1500 hours. Their age ranged from 35 to 49 years and their flight experience on helicopters ranged from 1400 to 4400 hours. Two pilots hold ratings for CH-47, AH-64, UH-72A and UH-60 models, while two pilots hold current ratings for types AS332/532 and the EC635, the military version of the EC135. In the following, the pilots are identified with letters from A to D.

4.2 Overview

Table 2 gives a summarized overview of all of the approaches. Out of these 24 approaches, 15 were considered successful due to the system showing reactions similar to simulation. These are marked with a bright background in Table 2. The three numbers in these cells indicate the distance at which the obstacle was detected, the minimal clearance of the rotor to the obstacle, and the skid height above ground (365 MSL) when reaching the hover location. Underlined values indicate significant deviations of more than 35% from the values expected from simulation.

Table 2: Summary of approaches during the campaign in Manching.

	Approach number								
Pilot	**1**	**2**	**3**	**4**	**5**	**6**	**7**	**8**	**9**
A	(F)	F	F	X	X	955 m 60 m 6 m	955 m 62 m 5 m	964 m 63 m 4 m	-
B	F	F	974 m 69 m 14 m	X	979 m 69 m 18 m	977 m 39 m 10 m	X	-	-
C	F	F	955 m 62 m 13 m	954 m 58 m 21 m	S	963 m 60 m 4 m	940 m 48 m 5 m	X	X
D	F	F	980 m 66 m 7 m	X	963 m 63 m 8 m	956 m 70 m 7 m	956 m 76 m 6 m	X	963 m 50 m 6 m

F = free approach
X = obstructed approach (GoAround)
S = special case (GPS drop-out)
_ = difference >35% compared to simulation

In nine approaches, marked with X and S in Table 2, the system reactions deviated from expectation, discussed separately in the results. During these flights, the system tried to avoid the truck vertically into an unintended high hover or did not propose a new flight path after an update. In these cases, the SP stopped descending and continued safely in level flight.

4.3 Symbology

Since the evaluation of the HMS/D symbology was the main focus, a simple primary flight display was configured on the EPs head-down display.

In Figure 15 a) to d), four different stages of the SferiAssist® symbology [20] during one of the approaches are shown in monochrome green on a black background. It was reproduced based on recorded flight state, path and LiDAR data, using the head-down version of the symbology.

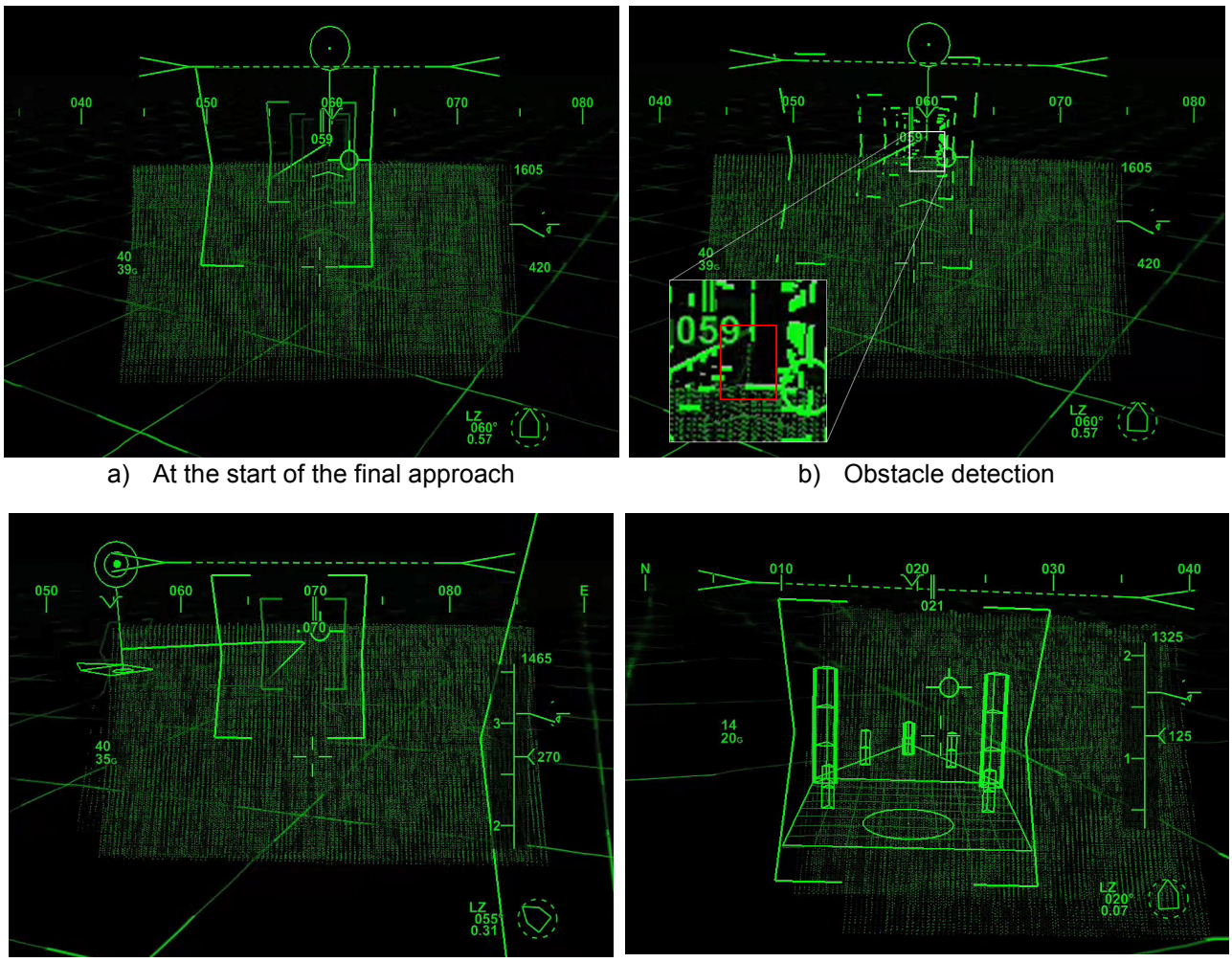

a) At the start of the final approach

b) Obstacle detection

c) After the path update

d) Before reaching the hover location.

Figure 15: SferiAssist® symbology at four points along one of the approach (Pilot C, Approach 2). Best viewed in color.

Figure 15 a) shows the symbology shortly after the start of the descending phase. The raw point clouds are shown as green dots with a persistence of two seconds above *a* geo-referenced grid. The active path is shown by a fading-in centerline and chevron symbols. The head-fixed overlay shows air- and ground speeds (left), a heading tape (up), the instantaneous flight path vector, a horizon line (up) and an indication of the vertical speed (right).

In Figure 15 b), the state of the symbology is shown, when the truck was detected the first time, indicated by the now changed line style of the chevron symbols. The “Lollipop” symbol above the horizon line indicates the location of the intended hover zone. Its orientation wih respect to the helicopters longitudinal axis is indicated on the lower right with numerical values for the distance in nautical miles and for the own heading. The magnification in the lower left of Figure 15 b) shows the LiDAR samples of the truck, hardly seen due to the small occupied area in the image at that distance.

Figure 15 c) shows the situation after the flight path was updated and the pilot followed the new tunnel. The chevron depiction changed to full line style again, indication no penetration of the check-volume. A landing zone indicator is shown at the end of the active path on the ground, with a slope indicator on top. The landing zone indication in the lower left has changed, since it was turned in flight path direction.

Finally, Figure 15 d) shows the hover symbology (“Doghouse”), shortly before reaching the hover location. The five small columns are 25 ft in height, the two large ones 75 ft. The vertical thick lines in the small middle and large outer columns indicate the own radar altitude. Note that the Lollipop symbol is now hidden to avoid visual cluttering.

Note that the path’s center line ends at a height above Mean Sea Level (MSL) as determined by the path planning module, shortly after the obstacle detection was raised. Compared to the simulated terrain, the real world terrain in Manching was

significantly lower (approx. 6 m) than the one contained in the database, as illustrated in Figure 17 a). Therefore, the flight path ended significantly higher than the intended 20 ft skid above ground.

5 RESULTS

In the following a detailed overview of the collected data during the flights is given. First, results and findings related to the LiDAR scans are discussed. Then, details concerning the path update procedure and the flight path for one of the approaches are given. Finally, the questionnaires are presented and discussed shortly.

5.1 LiDAR scan

As seen in Table 2, first detections occurred reproducibly in ranges around 950 m. A comparison of the truck from an aerial perspective as seen from the ACT/FHSs camera and a scanned point cloud is seen in Figure 16 a) and b). The structure of the truck can be clearly identified in Figure 16 b) due to the different spatial densities and occluded areas producing darker outlines.

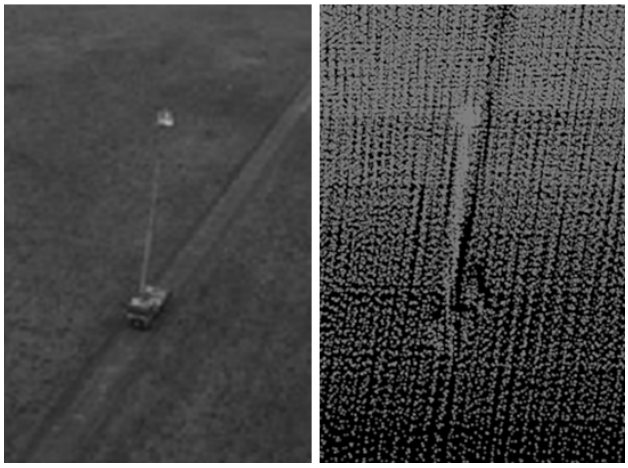

a) camera image b) point cloud

Figure 16: Truck seen from the ACT/FHS onboard TV camera vs. LiDAR scan, rendered from roughly the same perspective.

Note that the scan in Figure 16 b) was taken from one of the aborted approaches. The SP continued these approaches in straight and level flight and avoided the truck in a safe altitude. Therefore, it was in the sensors FOV for a longer period of time which resulted in point clouds with higher density in the area around the truck. However, when the lean structure of the truck first entered the FOV nearly 1000 m away, three cases occurred during the approaches, illustrated in Figure 17. The figure shows a view facing in flight direction with exaggerated points of the scan grid. In the best case, the truck was detected directly in its full height by one of the 95 rows of the LiDAR, seen in Figure 17 a).

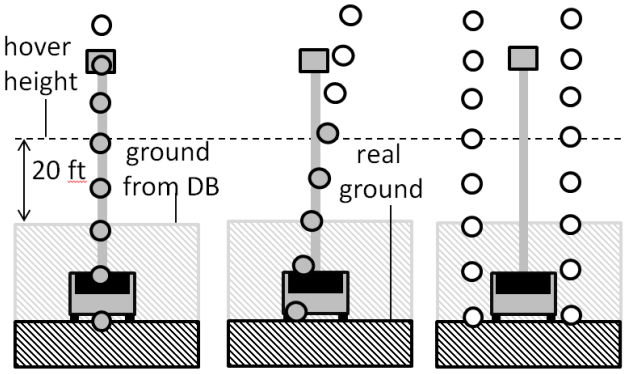

a) full detection b) skew detection c) no detection

Figure 17: Three cases of detection for the obstacle (scan pattern exaggerated)

Due to a non-leveled flight attitude, the sensors scan rows can also be slightly turned, scanning the truck not in its full height (Figure 17 b)). A third case occurred when the truck was between two scanning rows, as seen in Figure 17 c).

The systems reaction depends on the order in which these cases occur. Usually, full detections were the first to happen. In one approach however, the skew case happened first, resulting in a combination of go-above, then turn-right path updates.

5.2 Path updates

The result from the path update procedure for Pilot C's third approach is shown in Figure 18. Similar to Figure 11, the DSM (8 m grid) with the initial flight path is depicted in Figure 18 a), while Figure 18 b) shows the applied safety distances and the updated path.

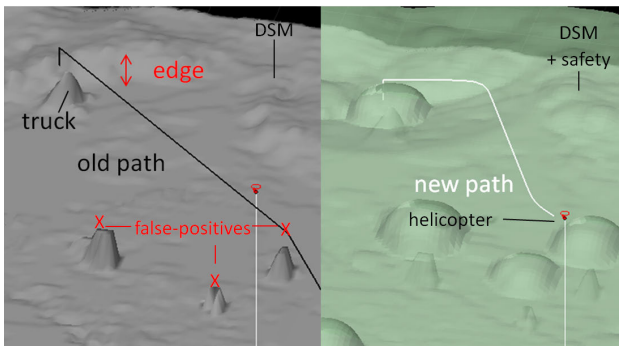

a) pre-update b) post-update

Figure 18: Path update process after an obstacle detection (Pilot C, Approach 2)

The truck is visible as clearly elevated point in the DSM in the upper left part of Figure 18 a). However, two things stand out compared to the same picture from simulation in Figure 11.

As already mentioned earlier, there was a difference in ground elevation from the a-priori database compared to the real world. In Figure 18 a), this is visible as edge, marked in the upper half. Since path updates were triggered by a detection of an obstacle only, the flight paths ended higher above the real ground. The consecutive mismatch in visual cues (end of path vs. doghouse) left two options for the pilots, each with its own drawback:

a) Staying inside the chevrons center. This resulted in a high hover (underlined in Table 2).
b) Leaving the path (chevrons center line) at some point during the final segment and following the landing symbology. This resulted in a steeper approach.

From the hover heights in Table 2 it can be concluded that Pilot A and Pilot D most probably chose option b) while Pilot B choose option a). As Pilot C reported during the debriefing, he changed his tunnel-following strategy after the third obstructed approach by leaving the tunnels center-line and orienting himself to the lower end of the chevrons.

In addition to Figure 18, a top view of the flight path for Pilot C's third approach is shown in Figure 19. Compared to the top view from simulation in Figure 12, the three intermitted obstacle detections in the lower left part is the most prominent visible difference. The two gaps in the detection indicate consecutive LiDAR frames with the truck being between two scanning rows (see Figure 17 c)).

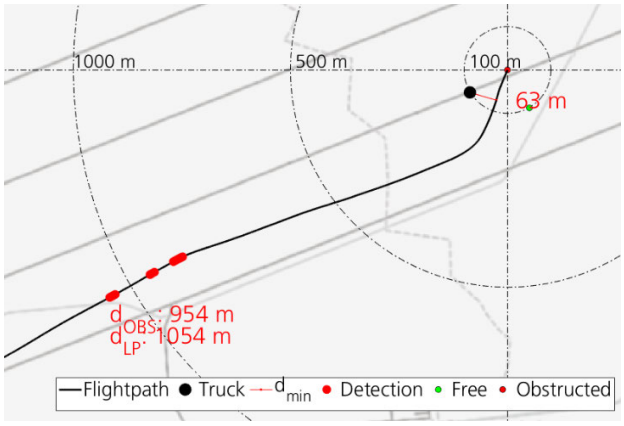

Figure 19: Top view of the flight path (Pilot C, Approach 2)

The obstacle clearance of more than 60 m was commented as comfortable after the flights. Nevertheless, the Pilots typically deviated from the tunnels center line (shortcutting) in the final turn to varying extent, leading to reduced clearances of less than 40 m and higher crew alertness in one case.

The mentioned Go-Around cases were a consequence of LiDAR returns which were most probably caused by large birds which were observed at the dropping area. Combined with a too sensitive DSM generation, these resulted in elevated points as seen in the lower half of Figure 18 a). In this particular case, these did not influence the path update.

But in the approaches marked with X in Table 2, one or more were present in the near vicinity to the hover location. As mentioned in section 2.2, the path planning displaces the hover point vertically in such cases in order to ensure the configured safety distances. From the pilot's point of view, the system suggested to avoid the truck vertically into a high hover, usually during a second path update following an expected lateral avoidance. Since this was an unexpected system behavior, the controls were handed over back to the SP safely.

5.3 Questionnaires

Multiple questionnaires were processed by the pilots. Subjective workload assessments with the NASA Task Load Index (TLX) [21] were answered during the flights after each test-point. Relevant results of two post-flight questionnaires are also shown in this section. First, the results of the NASA TLX questionnaire are given in Table 3.

Table 3: NASA TLX evaluation for free (F) and obstructed (O) approaches

	1	2	3	4	5	6	7
1 Mental Demand: How mentally demanding was the task?							
F		A,C	D		B		
O		A,C	D			B	
2 Physical Demand: How physically demanding was the task?							
F		B,C,D	A				
O		C,D	A	B			
3 Temporal Demand: How hurried or rushed was the pace of the task?							
F		A,C,D	B				
O		A	C	B,D			
4 Performance: How successful were you in accomplishing what you were asked to do?							
F		A,C,D	B				
O		A,C,D			B		
5 Effort: How hard did you have to work to accomplish your level of performance?							
F		C	A,D		B		
O		A,C	D		B		
6 Frustration: How insecure, discouraged, irritated, stressed and annoyed were you?							
F		C	B,D	A			
O		C,D		A	B		

The better end of the scale is always on the left side, increasing from low (1) to high (7). Note that in question 4, it increases from good (1) to poor (7) performance. The first row below the rating numbers includes the answers for the free (F) approaches, the second row for the obstructed (O) approaches respectively, allowing a direct comparison of both test points. Summarizing the results of both test points for each pilot in Table 3, the following points can be emphasized.

- While none of the pilots gave highest possible ratings, the majority of ratings is given on the better end of the scale.
- Pilots A,C and D gave at least equal ratings for the free and obstructed, curved approaches in categories 1,2,4 and 5.
- All pilots except Pilot A gave expectable higher ratings in category 5 (temporal demand), introduced by the obstacle detections and changing flight path.
- The better ratings of Pilot A in question 5 (effort) and Pilot D in question 6 (frustration) during the obstructed approaches can be explained by a higher degree of familiarization in the second half of the one-hour flight.
- Pilot B gave equally high ratings in the "Effort" category for both test-points, and higher ratings for the obstructed approaches in the other categories.

As mentioned previously in section 1.3, the experimental flight control laws of the ACT/FHS could not be used during the campaign, introducing a significant amount of workload for aircraft stabilization. Pilot B explicitly mentioned, that the overall poorer ratings in all of the questionnaires were strongly related to the unstable helicopter handling.

Situational awareness

The first post-flight questionnaire was related to the situational awareness for eight specific factors. First, the scale with a numeric rating from 1 to 10 and the corresponding verbalization is shown in Table 4.

Table 4: Situational awareness scale

Category	Rating	Meaning
High	1	Excellent
	2	Good
	3	Fair
Moderate	4	Minor deficiencies
	5	Moderate deficiencies
	6	Tolerable deficiencies
Low	7	Considerable pilot effort
	8	Intense pilot effort
	9	Extreme pilot effort
None	10	Lost awareness

The eight parameters the pilots were asked to rate are shown in the leftmost column of Table 5. The given answers are presented in the rightmost four columns, using the values as in Table 4.

Table 5: Results of situational awareness questionnaire

		Pilot			
	Rate your awareness of…	**A**	**B**	**C**	**D**
1	Height AGL & rate of descent	2	4	2	4
2	Speed & rate of closure	3	7	6	4
3	Heading	2	3	2	2
4	Landing/Hover position	2	5	3	3
5	Power margin	7	n/a	8	n/a
6	Drift lateral	2	4	2	2
7	Drift longitudinal	2	4	2	6
8	Terrain slope & roughness	3	4	n/a	3

Since there was no speed information attached to the tunnel-in-the-sky or information of power margin included in the HMI in general, the high ratings for speed, rate of closure and power margin are consistent. Points of improvement can be identified by the general poorer overall ratings of Pilot B and the moderate and low ratings of Pilot D in the height, speed and longitudinal drift parameters (1, 2 and 7). Apart from that, the leftover awareness ratings were given in the "High" category.

Paired comparison

The second post-flight questionnaire seen in Table 6 is focused on the way and amount of preferred

Table 6: Results of "Paired comparison" questionnaire

	←Higher−			Equal	−Higher→			
The amount of information presented was too little			A	B,C,D				The amount of information presented was too high
Preferred use of information displayed on HMD		B	A	C				Preferred use of information displayed on HDD/MFD
Preferred use of 3D symbology or imagery		B		C	A			Preferred use of 2D symbology
Preferred use of fused persistent information	C			A	B			Preferred use of real time sensor depiction
Preferred use of photorealistic display (pot. with augmentation)						B,C	A	Preferred use of SVS (pot. enhanced by real time sensor data)

information. A paired comparison is used to evaluate preferences with respect to five different factors.

The spread of answers in the middle three questions is quite large, leaving no clear conclusion about the general tendency. The distribution of answers in the first and last question however is more consistent. According to the answers, the amount of information presented to the pilot seems to be enough to fulfill the given task with workloads in the lower half of the NASA TLX workload scale. Additionally, synthetic vision elements are preferred over photorealistic depictions in the evaluated use case.

6 CONCLUSIONS

A multi-module system allowing deterministic avoidance of obstacles has been demonstrated in 15 of the 24 obstructed approaches without prior reconnaissance during the campaign. The main findings:

- The lean obstacle has been detected repeatedly in a distance of more than 950 m under clear VFR conditions.
- The evaluation flights yielded overall positive feedback of the system, although areas for improvement were named precisely by the four pilots.
- Issues regarding high hover states or Go-Arounds have been identified as a consequence of a difference in real-world vs. database terrain and the current LiDAR processing.
- The used path update procedure has shown to provide deterministic, lateral avoiding flight path updates.
- The temporarily missing stabilization of the ACT/FHS introduced an increased amount of workload, hence underlining the need of advanced flight controls in DVE.

Although the overall results of the evaluation are very promising from a technical point of view, the known scenery with a single raised obstacle under constant visual contact has limited operational relevance. The strength of active sensor systems lies in scenarios in which the systems range of perception exceeds the pilot's. In case path changes happen in these situations, an improved HMI is needed to communicate the systems decisions to the pilot.

7 FUTURE WORK

Solutions to most of the mentioned issues like missing cues for speed and torque, LiDAR data processing are straightforward initial next steps. Challenges introduced by phenomena at the border of the sensors FOV need to be addressed as well. In particular, these include partial detections, handling of significant differences of a-priori and sensed terrain and moving objects within the FOV.

Additionally, several points in terms of pilot interaction in different stages can be added, from line-of-sight selection of a hover location at the start of the procedure up to interactive flight path influence during the approach. In case of obstacles very close to the hover location, an automatic or manual displacement of the hover location to a nearby better solution should be addressed as well.

Further on, the combination of the evaluated system with further components of the ACT/FHSs including active sidesticks and experimental flight control laws up to automatic path following are potential next steps.

In the long term, more challenging obstacle sceneries need to be investigated. Especially when highly automated path changes under real DVE conditions shall be considered, the corresponding HMI should allow the pilot to immediately understand the systems reactions in order to generate the highest possible level of trust.

Acknowledgements

The authors like to thank all colleagues at the institute of Flight Experiments, Flight Guidance and Flight Systems, who were involved during the time-constrained preparation of the campaign. This work has been partially funded with the support of the Federal Office of Bundeswehr Equipment, Information Technology and In-Service Support (BAAINBw).

References

[1] Anon., "The Compendium Report: The US JHSAT Baseline of Helicopter Accident Analysis, Volume II, (CY2000, CY2001, CY2006)," US Joint Helicopter Safety Analysis Team, July 2011

[2] Anon., "EHEST Analysis of 2006-2010 European helicopter accidents", European Helicopter Safety Team, August 2015

[3] Van Donghen, N. "Final Report of NIAG SG167 on Helicopter Operations at Low Altitude Degraded

Visual Environment (DVE)," NIAG-D(2013)0014, AC/225(VL)D(2013)0001, July 2013

[4] Münsterer, T., Scheuch, J., Völschow, P., Strobel, M., Roth, M., Fadljevic, D., „Capability Comparison of Pilot Assistance Systems Based Solely on Terrain Databases Versus Sensor DB Fused Data Systems“, P*roc. SPIE* 9839, Degraded Visual Environments: Enhanced, Synthetic, and External Vision Solutions 2016, 983905, May 13, 2016

[5] Air Accident Investigation Unit Ireland, “Preliminary Report, Accident Sikorsky S-92A, EI-ICR, Black Rock, Co. Mayo, Ireland”, March 2017

[6] Drwiega, A., “US Army Working with NATO on DVE and Next Gen Rotorcraft”, Vertiflite, May/June 2017

[7] Szoboszlay, Z., Davis, B., Fujizawa, B., Minor, J., Osmon, M., Morford, Z. “Degraded Visual Environment Mitigation (DVE-M) Program, Yuma 2016 Flight Trials in Brownout”, American Helicopter Society 73rd Annual Forum & Technology Display, Forth Worth, Texas, USA, May 9-11, 2017

[8] Kaletka, J., Kurscheid, H., Butter, U., “FHS, the new research helicopter: ready for service”. Journal of Aerospace science and technology, 9 (5) (2005), p. 456-467

[9] Greiser, S., Lantzsch, R., Wolfram, J., Wartmann, J., Müllhäuser, M., Lüken, T., Döhler, U., Peinecke, N., „Results of the pilot assistance system `Assisted Low-Level Flight and Landing on unprepared Sites`obtained with the ACT/FHS research rotorcraft”, Aerospace Science and Technology, Vol. 45, p. 215-227, 2015,

[10] Duda, H., Gerlach, T., Advani, S., Potter, M., „Design of the DLR AVES Research Flight Simulator“, AIAA Modelling and Simulation (MST) Conference, August 19-22, 2013, Boston, MA, USA

[11] Peinecke, N., Döhler, H.-U., Korn, B., „Simulation of imaging radar using graphics hardware acceleration“, *Proc. SPIE* 6957, Enhanced and Synthetic Vision 2008, 69570L (April 15, 2008);

[12] Wolfram, J., Zimmermann, M., Klasen, S., Gestwa, M., „Design of an automatic Transition to Hover system“, German Aerospace Congress, Braunschweig, Germany, Sept. 13-15, 2016

[13] Eibert, M., Schäfer, C.H., Stich, H., „Laser-Radar Based Obstacle Avoidance System for Helicopters“, Proc. of the 17th European Rotorcraft Forum, Berlin, Germany, Sept. 24-27, 1991;

[14] Schulz, K.R., Scherbarth, S., Fabry, U., „Hellas: Obstacle Warning system for helicopters“, Proc. SPIE 4723, Laser Radar Technology and Applications VII, 29 July 2002

[15] Seidel, C., Samuelis, C., Wegner, M., Münsterer T., Rumpf T., Schwartz I. „Novel Approaches to helicopter obstacle warning“, *Proc. SPIE* 6214, Laser Radar Technology and Applications XI, 621406, May 19, 2006

[16] Stelmash, S., Münsterer, T., Kramper, P., Samuelis, C., Bühler, D., Wegner, M., Sheth, S. “Flight test results of lada brownout look-through capability”, Proc. SPIE 9471, Degraded Visual Environments: Enhanced, Synthetic, and External Vision Solutions 2015, 947106 Baltimore, MD, USA June 11, 2015

[17] Döhler, H.-U., Peinecke, N., “ALLFLight – Imaging sensors fused with Ladar data for moving obstacle detection”, Proceedings of 39th European Rotorcraft Forum, Sept. 03-06 2013, Moscow, Russia.

[18] Srikanth, M.B., Mathias, P.C., Naraajan, V., Naidu, P. and Poston, T. “Visibility volumes for interactive path optimization”, The visual computer, Vol. 24, No 7-9, 2008, pp. 635-647

[19] Zimmermann, M., “Flight test results of helicopter approaches with trajectory guidance based on in-flight acquired LIDAR data”, *Proc. SPIE* 9839, Degraded Visual Environments: Enhanced, Synthetic, and External Vision Solutions 2016, 983902, 2016

[20] Münsterer, T., Völschow, P., Singer, B., Strobel, M. and Kramper, P., “DVE flight test results of a sensor enhanced 3D conformal pilot support system,” *Proc. SPIE* 9471, Degraded Visual Environments: Enhanced, Synthetic, and External Vision Solutions 2015, 947106 Baltimore, MD, USA June 11, 2015

[21] Anon. “NASA Task Load Index V 1.0 Manual - Paper and Pencil Package”, Human Performance Research Group, NASA Ames Research Center, Moffet Field, California, 1986